Kinetics and Mechanism of Reductive Elimination of C−H Bonds from (μ-H)$_3$Ru$_3$(μ_3-CX)(CO)$_9$ Revisited: CO Associative, CO Independent, or CO Dissociative?

Fred J. Safarowic and Jerome B. Keister*

Department of Chemistry, University at Buffalo, State University of New York, Buffalo, New York 14260-3000

Received March 4, 1996[⊗]

The kinetics of the isomerizations of (μ-H)$_3$Ru$_3$(μ_3-CCO$_2$Me)(CO)$_9$ to (μ-H)$_2$Ru$_3$(μ_3-η^2-CHCO$_2$Me)(CO)$_9$ and of (μ-H)$_3$Ru$_3$(μ_3-CSEt)(CO)$_9$ to (μ-H)Ru$_3$(μ_3-η^2-CH$_2$SEt)(CO)$_9$, including the measurements of activation volumes, are reported. An earlier study of reductive elimination of CH$_3$X from H$_3$Ru$_3$(μ_3-CX)(CO)$_9$ found that the reaction was promoted by CO for X = Ph, Cl, and Et and was unaffected by CO pressure for X = CO$_2$Me. The activation volume $\Delta V^{\ddagger}$ for the intramolecular isomerization of (μ-H)$_3$Ru$_3$(μ_3-CCO$_2$Me)(CO)$_9$ to (μ-H)$_2$Ru$_3$(μ_3-η^2-CHCO$_2$Me)(CO)$_9$ was determined to be −0.3(0.7) cm^3/mol at 57.0 °C. For the isomerization of (μ-H)$_3$Ru$_3$(μ_3-CSEt)(CO)$_9$ to (μ-H)Ru$_3$(μ_3-η^2-CH$_2$SEt)(CO)$_9$, the rate is inhibited by CO; activation parameters ($\Delta H^{\ddagger}$=121(3) kJ/mol, $\Delta S^{\ddagger}$= +36(10) J/(mol K), $\Delta V^{\ddagger}$= +22.0(1.4) cm^3/mol) are consistent with a mechanism involving reversible CO dissociation prior to the rate-determining step but following an intramolecular rearrangement. The change in mechanism of reductive elimination of a C−H bond from CO associative to CO independent to CO dissociative is due to anchimeric assistance by the methylidyne substituent. These results may have relevance to C−H formation occurring on metal surfaces.

Introduction

Reductive elimination of the C−H bond from a transition-metal center is an elementary step in many metal-catalyzed reactions. The mechanism has been the subject of numerous studies.[1] However, few of these have concerned reductive eliminations from metal clusters. As metal clusters have been cited as models for the structural features associated with the binding of organic fragments to metal surfaces,[2] the mechanisms of reactions of these clusters are of interest with respect to analogies to surface-catalyzed processes.

Reductive elimination of CH$_3$X from (μ-H)$_3$Ru$_3$(μ_3-CX)(CO)$_9$ had been previously examined.[3] The rate of the reaction increases with increasing CO pressure to a saturation limit for X = Cl, Et, and Ph, but the rate is unaffected by CO pressure for X = CO$_2$Me. Additionally, inverse deuterium kinetic isotope effects were measured for X = Cl, Et, and Ph, but a k_H/k_D value of 1 was found for (μ-H)$_3$Ru$_3$(μ_3-CCO$_2$Me)(CO)$_9$. The change in mechanism was attributed to the coordinating ability of the ester functionality.

To further elucidate the nature of the reductive-elimination process, we have now determined the kinetics for isomerization of (μ-H)$_3$Ru$_3$(μ_3-CSEt)(CO)$_9$ to (μ-H)Ru$_3$(μ_3-η^2-CH$_2$SEt)(CO)$_9$,[4] a process involving reductive elimination of two C−H bonds (Figure 1). We have also measured the activation volume for the isomerization of (μ-H)$_3$Ru$_3$(μ_3-CCO$_2$Me)(CO)$_9$ to (μ-H)$_2$Ru$_3$(μ_3-η^2-CHCO$_2$Me)(CO)$_9$, involving a single C−H elimination (Figure 2). In combination with previous studies, these results show that C−H reductive elimination from (μ-H)$_3$Ru$_3$(μ_3-CX)(CO)$_9$ can occur by CO associative, CO dissociative, or CO independent pathways.

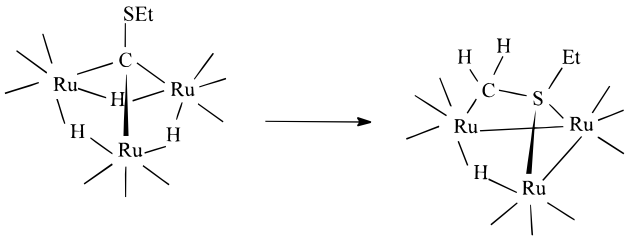

Figure 1. Structural changes in the rearrangement of (μ-H)$_3$Ru$_3$(μ_3-CSEt)(CO)$_9$ to (μ-H)Ru$_3$(μ_3-η^2-CH$_2$SEt)(CO)$_9$.

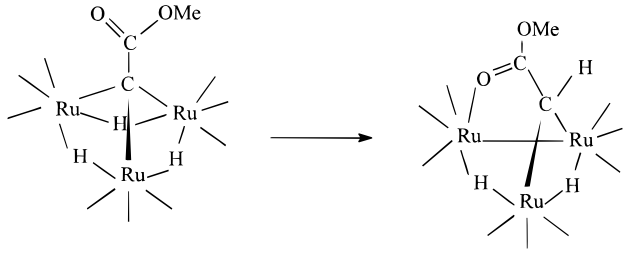

Figure 2. Structural changes in the rearrangement of (μ-H)$_3$Ru$_3$(μ_3-CCO$_2$Me)(CO)$_9$ to (μ-H)$_2$Ru$_3$(μ_3-η^2-CHCO$_2$Me)(CO)$_9$.

Experimental Section

The clusters (μ-H)$_3$Ru$_3$(μ_3-CCO$_2$Me)(CO)$_9$ [5] and (μ-H)$_3$Ru$_3$(μ_3-CSEt)(CO)$_9$ [4] were synthesized according to previously reported methods. Decane and heptane were used as received from Aldrich Chemical Co., Inc. Gases were uncertified (N$_2$)

[⊗] Abstract published in *Advance ACS Abstracts,* June 15, 1996.

(1) Collman, J. P.; Hegedus, L. S.; Norton, J. R.; Finke, R. G. *Principles and Applications of Organotransition Metal Chemistry*; University Science Books: Mill Valley, CA, 1987; Chapter 5.
(2) Muetterties, E. L.; Rhodin, T. N.; Band, E.; Brucker, C. F.; Pretzer, W. R. *Chem. Rev.* **1979**, *79*, 91.
(3) Duggan, T. P.; Golden, M. J.; Keister, J. B. *Organometallics* **1990**, *9*, 1656.
(4) Churchill, M. R.; Ziller, J. W.; Dalton, D. M.; Keister, J. B. *Organometallics* **1987**, *6*, 806.
(5) Keister, J. B.; Horling, T. L. *Inorg. Chem.* **1980**, *19*, 2304.

S0276-7333(96)00154-9 CCC: $12.00

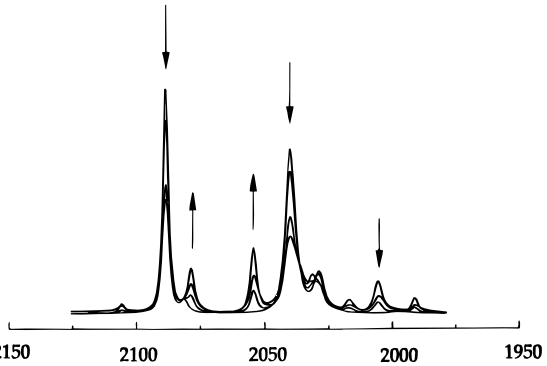

Figure 3. IR spectral monitoring of the progress of the rearrangement of $(\mu\text{-H})_3Ru_3(\mu_3\text{-CCO}_2\text{Me})(CO)_9$ to $(\mu\text{-H})_2Ru_3(\mu_3\text{-}\eta^2\text{-CHCO}_2\text{Me})(CO)_9$ from a run at 1021 atm.

Table 1. Rate Constants for the Isomerization of $(\mu\text{-H})_3Ru_3(\mu_3\text{-CCO}_2\text{Me})(CO)_9$ to $(\mu\text{-H})_2Ru_3(\mu_3\text{-CHCO}_2\text{Me})(CO)_9$ at 34−2041 atm and 57.0 °C

P (atm)	k (10^{-5} s^{-1})	P (atm)	k (10^{-5} s^{-1})
34	1.77(0.15)	2041	1.79(0.12)
34	1.79(0.13)	2041	1.9(0.2)
1021	1.85(0.08)		

CP grade (CO) and used as received. Infrared data were recorded on a Nicolet Magna 550 FT-IR spectrophotometer. Kinetic data were analyzed by computer-calculated linear least-squares fitting and were determined over 2−3 half-lives. Error limits are the standard errors, including the number of degrees of freedom via Student's t values; the 95% confidence limits can be obtained by doubling the reported uncertainties.

High-Pressure Measurements. The apparatus used for variable-pressure kinetic measurements was described previously.[6] The reaction solution was contained in a 10-cc hypodermic syringe which was immersed in the compression fluid filling a 40-cc high pressure reaction vessel, with the syringe needle sealed into the sample outlet assembly with an O-ring. Periodically the pressure was released and sampling was performed by insertion of a fine-bore needle through the sample outlet in the reaction vessel head and into the syringe. Then a 300 μL aliquot was withdrawn. Sampling required ca. 10 min. A 50:50 glycerol−water mixture was used for compression between 0 and 30 000 psi. Pressure was determined with a Heise gauge (precision ±20 psi).

Determination of the Activation Volume for the Isomerization of $(\mu\text{-H})_3Ru_3(\mu_3\text{-CCO}_2\text{Me})(CO)_9$. The kinetics at 1 atm pressure were previously reported.[3] In this work we determined the rate constants for isomerization at 57.0 °C and hydrostatic pressures of 34, 1021, and 2041 atm. $(\mu\text{-H})_3Ru_3(\mu_3\text{-CCO}_2\text{Me})(CO)_9$ (5 mg) was dissolved in 8 mL of decane (0.99 mM). The sample was loaded as described above, and the pressure vessel was submerged in an oil bath (temperature controlled (±0.5 °C) by a Haake C1 constant temperature circulator), was allowed to thermally equilibrate at 57.0 °C, and was then pressurized. The reaction was monitored over 3 half-lives by the change in the infrared absorption at 2090 cm^{-1} (Figure 3). The reaction is well-behaved, as demonstrated by the isosbestic points in the IR spectrum. Plots of −ln(absorbance) vs time are linear over 3 half-lives, as previously reported for this first-order process. Duplicate runs at 34 and at 2041 atm were conducted, with a single run at 1021 atm; the observed rate constants with associated standard errors are presented in Table 1. No significant pressure effect was noted. The value $\Delta V^{\ddagger}$ of −0.3(0.7) cm^3/mol was determined from the slope of the plot of RT ln(k) vs P (Figure 4A).

(6) (a) Paw, W. Ph.D. Thesis, University at Buffalo, 1995. (b) Paw, W.; Bower, D. K.; Bierdeman, D. J.; Keister, J. B.; Schulman, E. M. *J. Coord. Chem.*, in press.

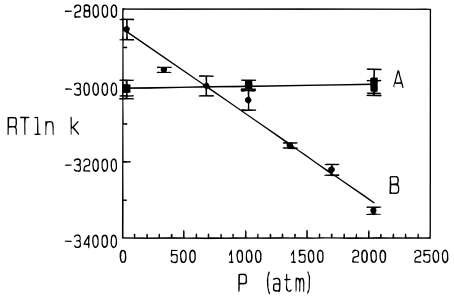

Figure 4. Plots of RT ln k vs P: (A) isomerization of $(\mu\text{-H})_3Ru_3(\mu_3\text{-CCO}_2\text{Me})(CO)_9$ to $(\mu\text{-H})_2Ru_3(\mu_3\text{-}\eta^2\text{-CHCO}_2\text{Me})(CO)_9$; (B) isomerization of $(\mu\text{-H})_3Ru_3(\mu_3\text{-CSEt})(CO)_9$ to $(\mu\text{-H})Ru_3(\mu_3\text{-}\eta^2\text{-CH}_2\text{SEt})(CO)_9$.

Kinetics of the Isomerization of $(\mu\text{-H})_3Ru_3(\mu_3\text{-CSEt})(CO)_9$. In decane solution, $(\mu\text{-H})_3Ru_3(\mu_3\text{-CSEt})(CO)_9$ irreversibly isomerizes at 1 atm and 50−80 °C to give $(\mu\text{-H})Ru_3(\mu_3\text{-}\eta^2\text{-CH}_2\text{SEt})(CO)_9$. At 50.0 °C isosbestic points are noted in the terminal carbonyl region of the infrared spectrum (Figure 5), indicating a quantitative reaction with no measurable quantity of intermediate formed during the reaction. Under a CO atmosphere the product decomposes to a mixture of $Ru(CO)_5$ and $Ru_3(CO)_{12}$; the rate of the decomposition increases with increasing CO pressure and at 50 °C and 2.7 atm is complete within 2 h. Consequently, isosbestic points are not observed for runs under a CO atmosphere.

The rate of isomerization of $(\mu\text{-H})_3Ru_3(\mu_3\text{-CSEt})(CO)_9$ at 1 atm and 50−80 °C was determined. $(\mu\text{-H})_3Ru_3(\mu_3\text{-CSEt})(CO)_9$ (10 mg) was dissolved in 10 mL of decane or THF (1.6 mM). The sample was placed in a thermostated cell (temperature controlled (±0.1 °C) by a Haake GH constant temperature bath) fitted with a condenser and nitrogen inlet. Aliquots were taken periodically over 3 half-lives, and the change in the infrared absorbance at 2079 cm^{-1} was determined (Figure 5). Plots of −ln(absorbance) vs time were linear, signifying a rate law that is first order in cluster concentration. Three runs were performed under each set of conditions (Table 2); the rate constants are reported as the average of the three, with the error limits as the larger of the standard deviation or the largest standard error of any of the individual runs. The rate of disappearance of $(\mu\text{-H})_3Ru_3(\mu_3\text{-CSEt})(CO)_9$ is inhibited by the presence of a CO atmosphere (Table 2), but the product $HRu_3(CH_2SEt)(CO)_9$ reacts further with CO to give $Ru(CO)_5$. From an Eyring plot of ln(k_{obs}/T) vs $1/T$ the activation parameters for the isomerization were determined to be $\Delta H^{\ddagger}$=121(3) kJ/mol (28.9(0.8) kcal/mol) and $\Delta S^{\ddagger}$= +36(10) J/(mol K) (9(2)cal/(mol K)). We were unable to prepare the deuterium-labeled compound $(\mu\text{-D})_3Ru_3(\mu_3\text{-CSEt})(CO)_9$ because of exchange of the label with silica gel; therefore, we were unable to determine the kinetic isotope effect for the isomerization.

The rate of the isomerization is faster in THF solution (k_{obs} = 1.29(0.07) × 10^{-4} s^{-1} at 50.0 °C) than in decane solution (1.5 × 10^{-5} s^{-1}).

Activation Volume for the Isomerization of $(\mu\text{-H})_3Ru_3(\mu_3\text{-CSEt})(CO)_9$. Measurements were conducted as described above, at 58.0 °C and using 1.2 mM heptane solutions. The change in infrared absorption at 2079 cm^{-1} was determined. One run at each of seven pressures was conducted; the observed rate constants, with associated standard errors, are presented in Table 3. The value of $\Delta V^{\ddagger}$ was determined to be +22.0(1.4) cm^3/mol, determined from the slope of the plot of RT ln(k) vs P (Figure 4B). The error limit is the computer-calculated standard error from the plot.

Kinetics of $AsPh_3$ Substitution on $(\mu\text{-H})_3Ru_3(\mu_3\text{-CSEt})(CO)_9$. A heptane solution of $H_3Ru_3(CSEt)(CO)_9$ (0.7−2.0 mM) was placed in a Schlenk flask under a nitrogen or carbon monoxide atmosphere, and this flask was immersed in a thermostated bath at 30.0 °C. Then $AsPh_3$ was added to the solution to give the desired concentration. After dissolution,

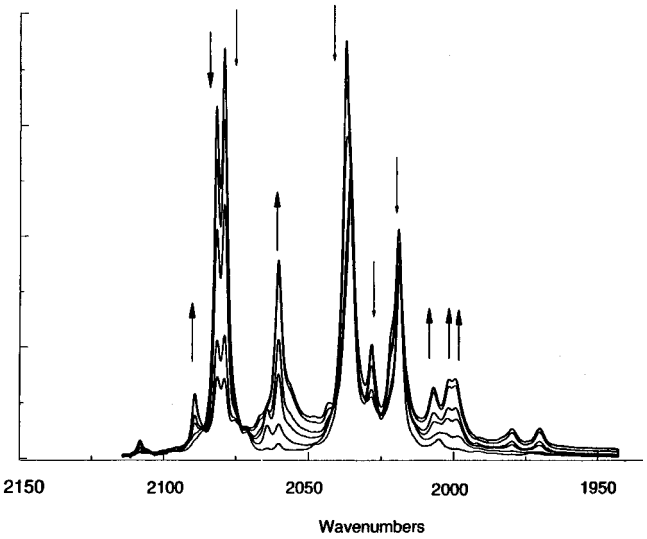

Figure 5. IR spectral monitoring of the progress of the rearrangement of $(\mu\text{-H})_3Ru_3(\mu_3\text{-CSEt})(CO)_9$ to $(\mu\text{-H})Ru_3(\mu_3\text{-}\eta^2\text{-}CH_2SEt)(CO)_9$ under 1 atm of nitrogen.

Table 2. Rate Constants for the Isomerization of $(\mu\text{-H})_3Ru_3(\mu_3\text{-CSEt})(CO)_9$ to $(\mu\text{-H})Ru_3(\mu_3\text{-}\eta^2\text{-}CH_2SEt)(CO)_9$ at 1 atm Pressure under Nitrogen or CO

T (°C)	*P*(N_2) (atm)	*P*(CO) (atm)	*k* (10^{-5} s^{-1})
50.0	1	0	1.5(0.7)
65.0	1	0	11(2)
65.0	0	1	4.2(0.2)
80.0	1	0	75(5)

Table 3. Rate Constants for the Isomerization of $(\mu\text{-H})_3Ru_3(\mu_3\text{-CSEt})(CO)_9$ to $(\mu\text{-H})Ru_3(\mu_3\text{-CH}_2SEt)(CO)_9$ at 58.0 °C and 34−2041 atm

P (atm)	*k* (10^{-5} s^{-1})	*P* (atm)	*k* (10^{-5} s^{-1})
34	3.1(0.3)	1361	1.04(0.03)
340	2.13(0.05)	1701	0.82(0.04)
681	1.8(0.2)	2041	0.56(0.02)
1021	1.60(0.15)		

Table 4. Rate Constants for Substitution by $AsPh_3$ on $(\mu\text{-H})_3Ru_3(\mu_3\text{-CSEt})(CO)_9$ at 30.0 °C

$[H_3Ru_3(CSEt)(CO)_9]_0$ (mM)	$[AsPh_3]$ (mM)	*P*(CO) (atm)	k_{obs} (10^{-4} s^{-1})
0.7	1.7	0	7.0(0.16)
	1.7	1	1.43(0.03)
2.0	17	0	5.4(0.2)
	17	1	5.3(0.3)

samples were taken at intervals for FT-IR analysis. Plots of ln(absorbance at 2108 cm^{-1}) vs time were linear over greater than 3 half-lives. Rate constants are given in Table 4.

Results and Discussion

As one of the most significant reactions in organometallic chemistry, reductive elimination of the C−H bond (and the microscopic reverse reaction, oxidative addition) from a transition-metal complex has been the subject of much study.[1] Relatively few studies of cluster systems have appeared. As metal clusters have been cited as models for the structural features associated with the binding of organic fragments to metal surfaces,[2] the potential relevance of the mechanisms of these clusters to surface-catalyzed processes makes such studies of general interest. In particular, the μ_3-alkylidyne moiety is well-established on a wide variety of metal surfaces.[7] Desorption of this fragment by C−H elimination may be modeled by the reductive-elimination reactions of $(\mu\text{-H})_3Ru_3(\mu_3\text{-CX})(CO)_9$.

The commonly acccepted mechanism for C−H reductive elimination from a single metal center involves a three-center transition state, forming a σ (or agostic) complex, which may have a significant lifetime.[8] Since agostic complexes tend to be comparatively stable in polymetallic systems (compared to mononuclear complexes), it is reasonable that the kinetics of reductive eliminations from clusters may differ in some respects from reductive eliminations involving a single metal center. The work reported herein demonstrates that the intramolecular coordinating ability of hydrocarbyl substituents can have a dramatic effect upon the mechanism of the elimination reaction, even in very closely related molecules.

Reductive elimination of CH_3X from $(\mu\text{-H})_3Ru_3(\mu_3\text{-CX})(CO)_9$ is one of the few examples of cluster-based C−H eliminations for which kinetic studies are possible.[3] Under a CO atmosphere reductive elimination of CH_3X occurs for X = Ph, Et, Cl, CO_2Me, and SEt. On the other hand, for X = OMe only reductive elimination of molecular hydrogen occurs. For X = Ph, Et, and Cl, the rate of elimination of CH_3X was found to be accelerated by higher pressures of CO (eq 1), and the inverse kinetic

$$\text{rate} = \frac{k_1k_3k_5[CO]}{k_2k_4 + (k_2 + k_3)k_5[CO]}[H_3Ru_3(CX)(CO)_9] \quad (1)$$

isotope effect (k_H/k_D = 0.46−0.64) was taken as an indication for the existence of a preequilibrium formation of an agostic intermediate. While this intermediate could not be observed, the analogs $[(\mu\text{-H})_3Ru_3(\mu_3\text{-}\eta^2\text{-HCR})(CO)_9]^+$ (R = Et, $CHPhCH_2Ph$) were prepared by protonation of the alkylidynes in triflic acid and were shown to undergo rapid reductive elimination.[9] The mechanism was proposed to involve reversible formation of an agostic C−H bond and dissociation of the agostic complex to generate a vacant coordination site, which is trapped by CO (Figure 6).

Under a CO atmosphere $(\mu\text{-H})_3Ru_3(\mu_3\text{-CCO}_2Me)(CO)_9$ eliminates methyl acetate, a process for which the rate was found to be independent of the CO partial pressure and the kinetic isotope effect was determined to be 1 within experimental error. The rate for this process is significantly faster than the rates for reductive eliminations from $(\mu\text{-H})_3Ru_3(\mu_3\text{-CX})(CO)_9$ (X = Et, Cl, Ph). However, pyrolysis in the absence of CO produces $(\mu\text{-H})_2Ru_3(\mu_3\text{-}\eta^2\text{-CHCO}_2Me)(CO)_9$ in quantitative yield (Figure 2).[10] The rate of this isomerization was found to be the same as the rate of reductive elimination of methyl acetate under a CO atmosphere, suggesting the same rate-determining step. Shapley and Strickland characterized the analogs $(\mu\text{-H})_2Os_3(\mu_3\text{-CHC(O)X})(CO)_9$ from pyrolyses of $(\mu\text{-H})_3Os_3(\mu_3\text{-CC(O)X})(CO)_9$ (X = OMe, NR_2);

(7) Representative examples: (a) Parmeter, J. E.; Hills, M. M.; Weinberg, W. H. *J. Am. Chem. Soc.* **1988**, *110*, 7952. (b) Kesmodel, L. L.; Dubois, L. H.; Somorjai, G. A. *J. Chem. Phys.* **1979**, *70*, 2180. (c) Marinova, Ts. S.; Kostov, K. L. *Surf. Sci.* **1987**, *181*, 573. (d) Levis, R.; Winograd, N.; DeLouise, L. A. *J. Am. Chem. Soc.* **1987**, *109*, 6873.

(8) Brookhart, M.; Green, M. L. H. *J. Organomet. Chem.* **1983**, *250*, 395.

(9) Bower, D. K.; Keister, J. B. *Organometallics* **1990**, *9*, 2321.

(10) Churchill, M. R.; Janik, T. S.; Duggan, T. P.; Keister, J. B. *Organometallics* **1987**, *6*, 799.

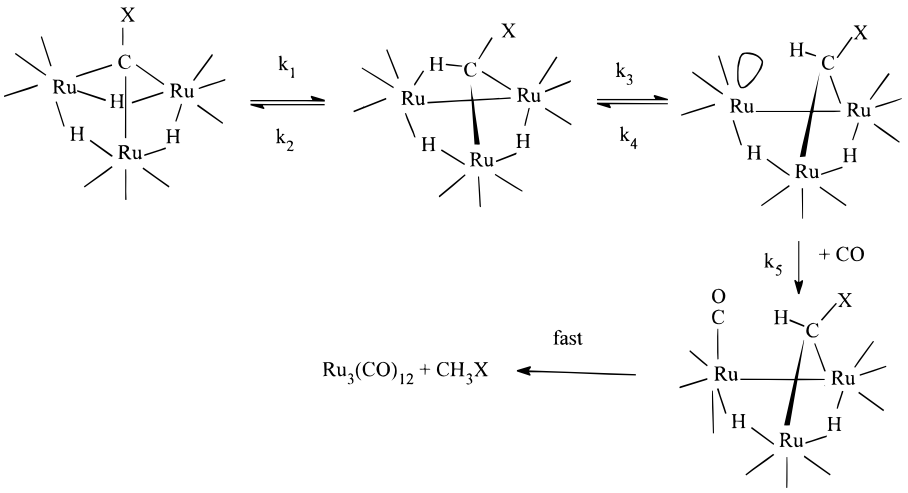

Figure 6. Proposed mechanism for reductive elimination of CH_3X from $(\mu\text{-H})_3Ru_3(\mu_3\text{-CX})(CO)_9$.

the amido derivative isomerizes ca. 30 times faster than the ester derivative.[11]

The faster rates for reductive elimination from alkylidynes having coordinating substituents such as C(O)OMe and $C(O)NR_2$, the zero-order dependence of the rate upon [CO], and the lack of a deuterium isotope effect indicates a different mechanism for isomerization/reductive elimination for $(\mu\text{-H})_3M_3(\mu_3\text{-CC(O)X})(CO)_9$. The limited information available for such a first-order process makes it difficult to learn much about the nature of the activated complex. We therefore sought to probe the volume change associated with the reaction. Activation volumes, $\Delta V^{\ddagger}$, for a number of organometallic reactions have been examined in recent years.[12a] The volume of activation of a reaction provides information complementary to that derived from the activation enthalpy and entropy. As $\Delta V^{\ddagger}$ can be frequently determined more precisely than the activation entropy, the activation volume may be more easily subjected to interpretation. The volume of activation, $\Delta V^{\ddagger}$, can be divided into two components: (1) the intrinsic volume change ($\Delta V^{\ddagger}_{int}$) which is related to changes in the van der Waals radii upon formation of the activated complex and (2) the volume change associated with the interaction of the solvent with reactant and transition state complex ($\Delta V^{\ddagger}_{solv}$).[12] In reactions where no significant solvent effect is observed, $\Delta V^{\ddagger}_{solv}$ may be considered to be small. In general, reactions involving bond breaking should have positive $\Delta V^{\ddagger}$ values, reactions involving bond making should show negative values of $\Delta V^{\ddagger}$, and reactions involving only changes in bond angles should have near-zero $\Delta V^{\ddagger}$. Similar generalizations hold for activation entropies, except that significantly negative $\Delta S^{\ddagger}$ and near-zero $\Delta V^{\ddagger}$ values have been found for some intramolecular rearrangements, such as trigonal-twist isomerizations and hydride fluxionality in clusters.

Isomerization of $(\mu\text{-H})_3Ru_3(\mu_3\text{-CCO}_2\text{Me})(CO)_9$ to $(\mu\text{-H})_2Ru_3(\mu_3\text{-}\eta^2\text{-CHCO}_2\text{Me})(CO)_9$. In this work we have determined that there is no measurable difference in volume between the starting cluster $(\mu\text{-H})_3Ru_3(\mu_3\text{-CCO}_2\text{Me})(CO)_9$ and the activated complex for the isomerization to $(\mu\text{-H})_2Ru_3(\mu_3\text{-CHCO}_2\text{Me})(CO)_9$ in decane solution. The isomerization of $(\mu\text{-H})_3Ru_3(\mu_3\text{-CCO}_2\text{Me})(CO)_9$ does not involve CO dissociation prior to the rate-determining step. Added CO has no effect upon the rate of reductive elimination, although the products are then $Ru_3(CO)_{12}$ and methyl acetate. The small value of $\Delta V_0^{\ddagger}$, −0.3(0.7) cm^3/mol, is consistent with an intramolecular process in which either there are no appreciable changes in bond lengths upon formation of the activated complex or there is coincidental compensation of bond breaking and bond formation. The entropy of activation is similarly close to zero (−0.8 J/(K mol)).[3] As hydride migration seems to cause very small volume changes, we cannot exclude the involvement of hydride migration in the rate-determining step. For comparison, hydride fluxionality on $H(\mu\text{-H})Os_3(CO)_{10}(PPh_3)$, involving intramolecular exchange of bridging and terminal hydride ligands, displays $\Delta V_0^{\ddagger} = -0.8(0.4)$ cm^3/mol ($\Delta S^{\ddagger}$ −54 J/(K mol)), and the value of $\Delta V_0^{\ddagger}$ for exchange between bridging hydrides of $(\mu\text{-H})_2Ru_3(\mu\text{-CHCO}_2\text{Me})(CO)_9$ is +4.1(0.3) cm^3/mol ($\Delta S^{\ddagger}$ −40 J/(K mol)).[13] The acceleration in rate of isomerization with the increasing coordinating ability of the methylidyne substituent suggests that carboxyl coordination stabilizes the transition state, but the near-zero values for the activation volume and entropy suggest the involvement of compensating bond cleavage. The previously proposed mechanism shown in Figure 7, which involves simultaneous bond cleavage and formation, cannot be discounted.[3,11] Too little information is available to draw a conclusion concerning the nature of the activated complex. The first-order rate law, the lack of CO dependence, and the small magnitude of the activation volume would appear to rule out ligand dissociation (which should have a substantially positive $\Delta V_0^{\ddagger}$), CO association, or bimolecular hydrogen transfer (the last two should show substantially negative $\Delta V_0^{\ddagger}$ values).

Isomerization of $(\mu\text{-H})_3Ru_3(\mu_3\text{-CSEt})(CO)_9$ to $(\mu\text{-H})Ru_3(\mu_3\text{-}\eta^2\text{-CH}_2\text{SEt})(CO)_9$. A different mechanism must occur for the rearrangement of $(\mu\text{-H})_3Ru_3(\mu_3\text{-CSEt})(CO)_9$ to $(\mu\text{-H})Ru_3(\mu_3\text{-}\eta^2\text{-CH}_2\text{SEt})(CO)_9$. The kinetic results obtained are consistent with the mechanism

(11) Strickland, D. A.; Shapley, J. R. *J. Organomet. Chem.* **1991**, *401*, 187.

(12) (a) van Eldik, R.; Asano, T.; le Noble, W. J. *Chem. Rev.* **1989**, *89*, 549. (b) van Eldik, R. *Inorganic High Pressure Chemistry: Kinetics and Mechanism*; Elsevier: Amsterdam, 1986.

(13) Keister, J. B.; Frey, U.; Zbinden, D.; Merbach, A. E. *Organometallics* **1991**, *10*, 1497.

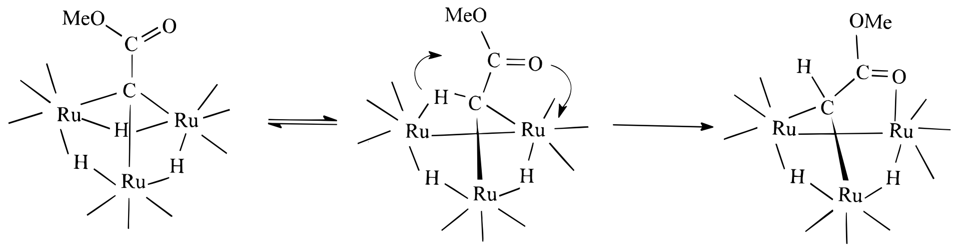

Figure 7. Proposed mechanism for isomerization of $(\mu\text{-H})_3Ru_3(\mu_3\text{-CCO}_2Me)(CO)_9$ to $(\mu\text{-H})_2Ru_3(\mu_3\text{-}\eta^2\text{-CHCO}_2Me)(CO)_9$.

$$H_3Ru_3(CO)_9(\mu_3\text{-CSEt}) \underset{k_2}{\overset{k_1}{\rightleftharpoons}} \text{intermediate A} \quad (2)$$

$$\text{intermediate A} \underset{k_4}{\overset{k_3}{\rightleftharpoons}} \text{intermediate B} + CO \quad (3)$$

$$\text{intermediate B} \xrightarrow{k_5} \text{intermediate C} \quad (4)$$

$$\text{intermediate C} + CO \xrightarrow{\text{fast}} HRu_3(CO)_9(CH_2SEt) \quad (5)$$

The magnitude of the inhibition of the rate by an atmosphere of CO is comparable to inhibitions of ligand substitutions involving CO dissociation. The entropy of activation ($\Delta S^{\ddagger} = +36$ J/(mol K)) and activation volume ($\Delta V_0^{\ddagger} = +22.0(1.4)$ cm^3/mol) are also typical for a CO dissociative mechanism. Examples of activation volumes for CO dissociation as the rate-determining step in ligand substitution include substitution on $[PPN][HRu_3(CO)_{11}]$ (+21.2 cm^3/mol), $Ru_3(CO)_{10}(P(OMe)_3)(CO_2Me)^-$ (+24 cm^3/mol),[14] and $Mn(CO)_5Cl$ (+20.6(0.4) cm^3/mol).[15] A lower value for hydrogenation of $HRu_3(\mu\text{-COMe})(CO)_{10}$ (+9.6 cm^3/mol), which occurs via CO dissociation, was attributed in part to rearrangement accompanying CO dissociation.[16]

However, the kinetics are inconsistent with CO dissociation from $(\mu\text{-H})_3Ru_3(\mu_3\text{-CSEt})(CO)_9$ itself. Ligand substitution on $(\mu\text{-H})_3Ru_3(\mu_3\text{-CX})(CO)_9$ (X = OMe, Me, Cl, Ph) has been examined previously and was found to involve rate-limiting CO dissociation.[17] To verify that the kinetics of substitution on $(\mu\text{-H})_3Ru_3(\mu_3\text{-CSEt})(CO)_9$ were comparable, we examined the rate of substitution on this cluster by $AsPh_3$, a poor nucleophile. The rate constant at 30.0 °C is similar to that found for other alkylidynes. These data establish the effect of the methylidyne substituent upon the rate of CO dissociation from $(\mu\text{-H})_3Ru_3(\mu_3\text{-CX})(CO)_9$ as (k at 303 K): X = OMe (1.5×10^{-3} s^{-1}) > SEt (5.4×10^{-4} s^{-1}) > Me (1.0×10^{-4} s^{-1}) ≈ Cl (8.9×10^{-5} s^{-1}) > Ph (3.7×10^{-5} s^{-1}). The rate constant is independent of $AsPh_3$ concentration and is unaffected under 1 atm of CO (concentration in heptane 1.8 mM at 25 °C) at 17 mM $AsPh_3$, but at 1.7 mM the reaction is inhibited by CO, indicating that the mechanism of substitution involves reversible CO dissociation. Thus, CO dissociation from $(\mu\text{-H})_3Ru_3(\mu_3\text{-CSEt})(CO)_9$ is much faster than the CO dissociation involved in the isomerization mechanism. It is likely that isomerization preceding CO dissociation is required to place the sulfur atom in a position geometrically favorable for coordination. CO dissociation from $(\mu\text{-H})_3Ru_3(\mu_3\text{-COMe})(CO)_7(PPh_3)_2$ occurs preferentially from the axial site trans to the Ru-C bond.[18] A number of possible structures for intermediates A and B can be proposed, given the plethora of intramolecular rearrangements of clusters. In addition to the observed rate law, any proposed mechanism must also account for the change in kinetics with the nature of the methylidyne substituent. Two possible mechanisms are shown in Figures 8 and 9. For either, the rate law, derived using the steady-state appoximation, is given by eq 10 and the limiting rate constant at low CO pressure and with $k_2 \gg k_3$ (for fast preequilibria) is shown in eq 11 (see below).

Reversible Hydride Migration Preceding CO Dissociation. Migration of a hydride to form an agostic Ru−H−C bond is a very reasonable equilibrium step preceding CO dissociation (Figure 8). Formation of an agostic bond in these types of isomerizations has been postulated previously to have a low activation energy. Reversible and rapid tautomeric equilibria between μ-hydride and agostic hydrogen have been established for a number of clusters. Shapley and co-workers measured the rate constant for exchange of hydride and methylidyne protons of $H_3Ru_3(\mu_3\text{-CH})(CO)_9$, presumably via Ru−H−Ru to Ru−H−C tautomerism, to be 1.1×10^{-2} s^{-1} at 34 °C.[19] Shapley also established a rapid equilibrium for eq 6.[20] Fehlner and co-workers established rapid equilibria for tautomerizations in eqs 7−9.[21,22]

$$H_2Os_3(\mu\text{-CH}_2)(CO)_{10} \rightleftharpoons HOs_3(\mu\text{-}\eta^2\text{-HCCH}_2)(CO)_{10} \quad (6)$$

$$H_2Fe_3(\mu_3\text{-}\eta^2\text{-HCH})(CO)_9 \rightleftharpoons HFe_3(\mu_3\text{-}\eta^3\text{-H}_2CH)(CO)_9 \quad (7)$$

$$H_3Fe_3(\mu_3\text{-CH})(CO)_9 \rightleftharpoons H_2Fe_3(\mu\text{-}\eta^2\text{-HCH})(CO)_9 \quad (8)$$

$$HFeCo_2(\mu_3\text{-CR})(CO)_9 \rightleftharpoons FeCo_2(\mu_3\text{-}\eta^2\text{-HCR})(CO)_9 \quad (9)$$

The equilibrium constant for the tautomerization has been shown to be affected by the identity of the metal atoms and the substituents on carbon. The effect of the alkylidyne substituent appears to be primarily steric in origin, as the equilibrium constant for eq 9 decreases

(14) Taube, D. J.; van Eldik, R.; Ford, P. C. *Organometallics* **1987**, *6*, 125.
(15) Schmidt, G.; Paulus, H.; van Eldik, R.; Elias, H. *Inorg. Chem.* **1988**, *27*, 3211.
(16) Anhaus, J.; Bajaj, H. C.; van Eldik, R.; Nevinger, L. R.; Keister, J. B. *Organometallics* **1989**, *8*, 2903.
(17) Abdul Rahman, Z.; Beanan, L. R.; Bavaro, L. M.; Modi, S. P.; Keister, J. B.; Churchill, M. R. *J. Organomet. Chem.* **1984**, *263*, 75.
(18) Feighery, W. G.; Yao, H.; Allendoerfer, R. D.; Keister, J. B. Manuscript in preparation.
(19) VanderVelde, D. G.; Holmgren, J. S.; Shapley, J. R. *Inorg. Chem.* **1987**, *26*, 3077.
(20) (a) Calvert, R. B.; Shapley, J. R. *J. Am. Chem. Soc.* **1977**, *99*, 5225. (b) Cree-Uchiyama, M.; Shapley, J. R.; St. George, G. M. *J. Am. Chem. Soc.* **1986**, *108*, 1316.
(21) Dutta, T. K.; Vites, J. C.; Jacobsen, G. B.; Fehlner, T. P. *Organometallics* **1987**, *6*, 842.
(22) Barreto, R. D.; Puga, J.; Fehlner, T. P. *Organometallics* **1990**, *9*, 662.

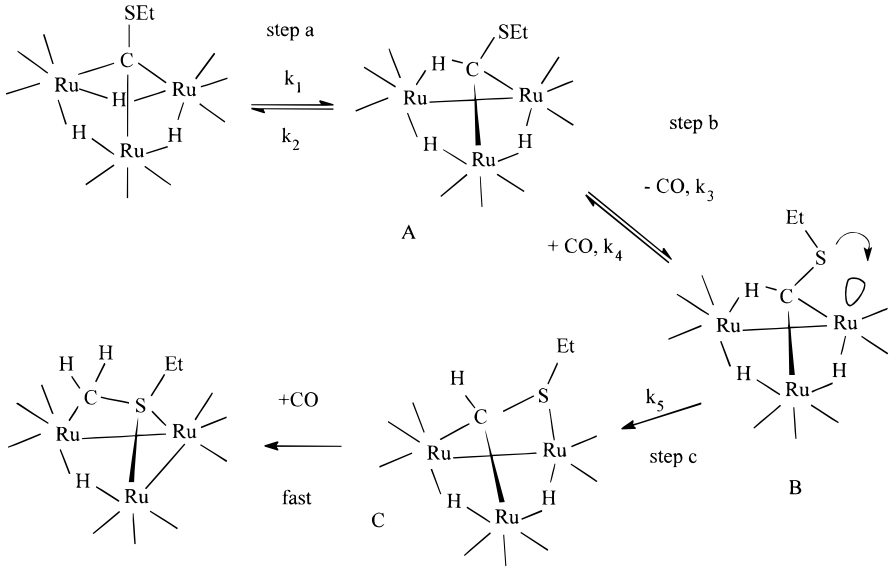

Figure 8. Proposed mechanism for isomerization of $(\mu\text{-H})_3Ru_3(\mu_3\text{-CSEt})(CO)_9$ to $(\mu\text{-H})Ru_3(\mu_3\text{-}\eta^2\text{-}CH_2SEt)(CO)_9$ involving a RuHRu to RuHC tautomerization.

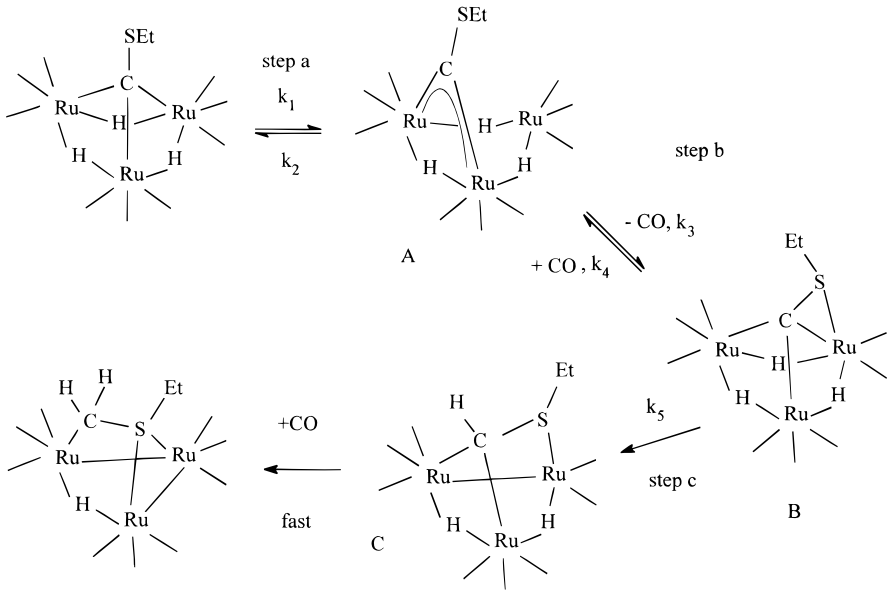

Figure 9. Proposed mechanism for isomerization of $(\mu\text{-H})_3Ru_3(\mu_3\text{-CSEt})(CO)_9$ to $(\mu\text{-H})Ru_3(\mu_3\text{-}\eta^2\text{-}CH_2SEt)(CO)_9$ involving a μ_3-CSEt to μ-CSEt isomerization.

in the sequence R = H > Me > Ph.[22] The equilibrium constant is also affected by the difference in electronegativities between carbon (or other capping atom) and the metals.[23]

The mechanism in Figure 8 is based upon the proposed mechanism of reductive elimination of CH_3X from $(\mu\text{-H})_3Ru_3(\mu_3\text{-CX})(CO)_9$ (X = Cl, Ph, Et). The isomerization of $(\mu\text{-H})_3Ru_3(\mu_3\text{-CSEt})(CO)_9$ is proposed to involve the reversible formation of an agostic Ru−H−C bond (eq 2 and Figure 8, step a) and reversible (in the presence of added CO) CO dissociation (eq 3 and Figure 8, step b), followed by the rate-determining step (eq 4), which is proposed to be Ru−H cleavage (Figure 8, step c). The ability of sulfur to coordinate to the vacant site of intermediate B promotes cleavage of the agostic bond. The second C−H elimination is proposed to be faster than the first; arguments supporting increasing rates for sequential C−H eliminations have been presented previously.[3] On the basis of prior studies of equilibria involving hydride−agostic hydrogen tautomerizations, it seems that the equilibrium in step a of Figure 8 should be rapid compared with the very slow rate of the overall reaction. Under our experimental conditions, the rate of isomerization is given by eq 10. In the absence of a CO atmosphere and since k_2 is expected to be much greater than k_3, k_{obs} is given by eq 11, and the activation entropy and volume will primarily reflect the contributions of k_3 for CO dissociation.

$$\text{rate} = \frac{k_1 k_3 k_5}{k_3 k_5 + k_2 k_5 + k_2 k_4[\text{CO}]}[H_3Ru_3(CSEt)(CO)_9] \tag{10}$$

$$k_{obs} = \frac{k_1 k_3}{k_2} \tag{11}$$

For clusters with noncoordinating methylidyne substituents, CO dissociation in step b, while still rapid,

(23) Fehlner, T. P. *Polyhedron* **1990**, *9*, 1955.

does not provide a route to reductive elimination. Agostic bond cleavage is reversible unless the unsaturated intermediate thus produced is trapped by added CO.

Reversible Methylidyne Migration Preceding CO Dissociation. The mechanism proposed in Figure 9 is suggested by the mechanism of reductive elimination of molecular hydrogen from $H_3Ru_3(\mu_3\text{-COMe})(CO)_9$ under CO, forming $HRu_3(\mu\text{-COMe})(CO)_{10}$ (eq 12).[24]

$$(\mu\text{-H})_3Ru_3(\mu_3\text{-COMe})(CO)_9 + CO \rightarrow (\mu\text{-H})Ru_3(\mu\text{-COMe})(CO)_{10} + H_2 \quad (12)$$

Hydrogen elimination is favored over C−H elimination by π-donor methylidyne substituents OMe and NR_2. The rationalization of the importance of π donor character for hydrogen elimination is that π donation from the methylidyne substituent to the methylidyne carbon stabilizes the μ-CX bonding mode over the μ_3-CX mode.[25] The SEt moiety also has significant π-donor character. If intermediate A contains a μ-CSEt substituent, H_2 elimination to $HRu_3(\mu\text{-CSEt})(CO)_9$ and ultimately $HRu_3(\mu\text{-CSEt})(CO)_{10}$ could compete with C−H elimination, leading to $HRu_3(\mu_3\text{-}\eta^2\text{-}CH_2SEt)(CO)_9$. However, CO dissociation is generally more favorable than H_2 elimination from clusters; formation of intermediate B by CO dissociation could also result in the $\mu_3\text{-}\eta^2$-CSEt ligand, as the sulfur donor atom occupies the vacant coordination site. An analogous structure was proposed for the intermediate in the hydrogen elimination, $HRu_3(\mu_3\text{-}\eta^2\text{-COMe})(CO)_9$, and several stable analogs such as $H_2Os_3(\mu_3\text{-}\eta^2\text{-}CCH_2)(CO)_9$ and $HRu_3(\mu_3\text{-}\eta^2\text{-}PPh_2)(CO)_9$ have been previously reported. The rate constant for CO dissociation from intermediate A (k_3; Figure 9) would be expected to be much smaller than the rate constant for the regeneration of the starting material from intermediate A (k_2; Figure 9). The primary contribution to $\Delta V^{\ddagger}$ is due to CO dissociation. In the absence of a coordinating methylidyne substituent to trap the vacant coordination site of intermediate A, no C−H elimination would occur by this route.

The most intriguing aspect concerning these clusters is the change in the mechanism of C−H elimination from CO associative to CO independent to CO dissociative with the identity of the methylidyne substituent. For $(\mu\text{-H})_3Ru_3(\mu_3\text{-CX})(CO)_9$ (X = Et, Cl, Ph) the methylidyne substituent has no appreciable coordinating ability and no appreciable π-donor character. Formation of the agostic complex and dissociation of the Ru−H−C bond is reversible unless CO is present to trap the unsaturated intermediate, thus giving rise to an increase in rate with [CO] to the limiting value for dissociation of the agostic bond. For $(\mu\text{-H})_3Ru_3(\mu_3\text{-}CCO_2\text{-Me})(CO)_9$, a favorable geometry allows the acyl group to promote dissociation of the agostic complex without the involvement of CO, since the rate of reductive elimination is much faster than the limiting rates obtained at high CO pressure for the noncoordinating methylidyne substituents.

While we had earlier proposed the same explanation, coordination of the SEt substituent promoting C−H elimination without change in CO coordination, our results now discount this. Involvement of sulfur in stabilizing the transition state for C−H elimination requires prior CO dissociation. This situation may differ from that for the ester analog because of the ability of the CO_2Me moiety (with an additional atomic spacer between the carbon and the donor atom) to attain a geometry more favorable for interaction with the Ru atom. What is clear is that the change in mechanism is not due to a faster rate of CO dissociation for $H_3Ru_3(\mu_3\text{-CSEt})(CO)_9$ compared with the other alkylidyne clusters. Ligand substitution rates via CO dissociation for all of these clusters are faster than the rates of reductive eliminations.[17] The ability of the SEt moiety to provide an alternative path for reductive elimination may be due to (1) the superior coordinating ability of sulfur to ruthenium and to (2) the strength of the C−S π bond, which stabilizes the μ-CSEt geometry relative to the μ_3-CSEt geometry.

For intramolecular rearrangements of this sort which involve anchimeric assistance by pendant groups, geometrical factors will be of primary importance. Further studies will investigate the role of alkylidyne chain length and donor atom in the promotion of these reductive eliminations.

Acknowledgment. This work was supported by the National Science Foundation through Grant No. CHE9213695. We thank Professors Rudi van Eldik (University of Erlanger-Nürnberg) and André Merbach (University of Lausanne) for valuable collaborations which taught J.B.K. the application of high-pressure measurements.

OM960154G

(24) (a) Dalton, D. M.; Barnett, D. J.; Duggan, T. P.; Keister, J. B.; Malik, P. T.; Modi, S. P.; Shaffer, M. R.; Smesko, S. A. *Organometallics* **1985**, *4*, 1854. (b) Bavaro, L. M.; Montangero, P.; Keister, J. B. *J. Am. Chem. Soc.* **1983**, *105*, 4977.

(25) Keister, J. B. *Polyhedron* **1988**, *7*, 847.